МАТЕМАТИЧНЕ МОДЕЛЮВАННЯ ФІЗИЧНИХ І ТЕХНОЛОГІЧНИХ ПРОЦЕСІВ І ТЕХНІЧНИХ СИСТЕМ

УДК 621.383.51:621.791.311

Ye.A. BAGANOV, V.O. GRAMOV
Kherson National Technical University

SIMULATION OF SPOT SOLDERING PROCESS FOR CRYSTALLINE SILICON SOLAR CELLS

In the paper the simulation of spot soldering process of interconnecting electrical conductive ribbon to the crystalline solar cells. The approach for calculation of soldering system speed depending on system heat power that provides low levels of overheating without solving of inverse heat conduction problem is suggested. Soldering system speed and its initial delay depending on system heat power was obtained.

Keywords: Solar cell, Soldering, Simulation

Є.О. БАГАНОВ, В.О. ГРАМОВ
Херсонський національний технічний університета

МОДЕЛЮВАННЯ ПРОЦЕСУ ТОЧКОВОЇ ПАЙКИ КРИСТАЛІЧНИХ КРЕМНІЙОВИХ СОНЯЧНИХ ЕЛЕМЕНТІВ

В роботі проведено математичне моделювання процесу точкової пайки з'єднувальних струмопровідних шин до монокристалічних кремнієвих сонячних елементів. Запропоновано підхід розрахунку швидкості проходу паяльної системи в залежності від її потужності для зменшення величини перегріву системи без розв'язання зворотної теплової задачі. Визначені швидкості проходу паяльної системи та її початкова затримка в залежності від потужності системи.

Ключові слова: сонячний елемент, пайка, моделювання.

Е.А. БАГАНОВ, В.А. ГРАМОВ
Херсонский национальный технический університет

МОДЕЛИРОВАНИЕ ПРОЦЕССА ТОЧЕЧНОЙ ПАЙКИ КРИСТАЛЛИЧЕСКИХ КРЕМНИЕВЫХ СОЛНЕЧНЫХ ЭЛЕМЕНТОВ

В работе проведено математическое моделирование процесса точечной пайки соединительных токопроводящих шин к монокристаллическим кремниевым солнечным элементам. Предложен подход расчета скорости прохода паяльной системы в зависимости от ее мощности для уменьшения величины перегрева солнечного элемента без решения обратной тепловой задачи. Определены скорости прохода паяльной системы и ее начальная задержка в зависимости от мощности системы.

Ключевые слова: солнечный элемент, пайка, моделирование.

Formulation of the problem

Crystalline silicon solar module is the critical component of photovoltaic generation system. In the process of crystalline silicon solar module production, the crystalline silicon solar cells (SCs) are interconnected into complete string. The cells in each string are electrically connected in series by interconnecting a tin-coated copper ribbon between the front of one cell and the back of the adjacent cell. The ribbon is bonded to the bus bar of the cells typically through soldering [1, 2]. This process in the assembly of SCs in PV modules has the advantage of yielding products, which possess high reliability at minimal production cost [3].

However, during the soldering operation, the cell and the ribbon are heated up to a high temperature near 200°C depending on solder type [4]. Differences in the thermal and mechanical properties of the silicon used in SC and metal ribbon cause the thermal deformation and the residual stress around the bonding area when the system is cooling down [5-8]. With time, it results in cracks occurrence and reduce of power output [5, 6].

Analysis of last investigations and publications

The standard soldering process provides heating and interconnection of SCs along its full length. Such operation leads to high levels of shear stress after cooling down [9]. One of possible ways of stress decreasing is

the use of spot soldering with a local heating of the ribbon-cell interface [9]. Two spot soldering techniques are suitable for SCs connection. There are soldering by a soldering iron tips and by a laser. The last one is more perspective due to possibility of accurate power control of the laser beam, high speed of laser soldering system and absence of the appliance of mechanical stress [10].

At this case, a controlled heating time and temperature are needed at the solder joint to form a high-quality intermetallic layer. In [10] it was shown that during laser soldering process the occurrence of cracks increases with increasing of peak temperature. It is coincide with results of [9] where claimed that precise control of time of soldering and decrease of temperature reduce the possibility of forming micro-cracks in the SCs.

The values of temperature peaks are dependent on two main parameters that are the speed of the soldering system and its heat power. To control the temperature during the soldering and predict appropriate process parameters the simulation is usually used [10, 11 – 13].

However, the direct calculations of temperature field dependence on several intensities and/or speeds have taken place only. There are no results and approaches to calculate power and speed dependences on time, which provides minimal temperature peaks in soldering zone during soldering process.

The purpose of the investigation

The purpose of the investigation is to develop an approach for prediction of power and speed dependences in time for spot soldering system during interconnection of crystalline silicon SC.

Statement of the basic material of the investigation

Conventionally SC has two bus bars (Fig.1). Soldering system realizes the soldering process of both bus bars simultaneously. Hence the vertical symmetry axis of SC is, at the same time, the symmetry axis for temperature field. Physically it corresponds to an absence of heat fluxes between left and right parts of SC.

Taking into consideration the thickness of modern SCs that is about 150-300 μm with in-plane dimensions of 156 mm the thermal fluxes from SC flanks can be neglected. Hence, thermal field has two additional symmetry axis that are coincides with symmetry axis of copper ribbons. That is why only one quarter of SC (hatched part in Fig. 1) was taken for simulation.

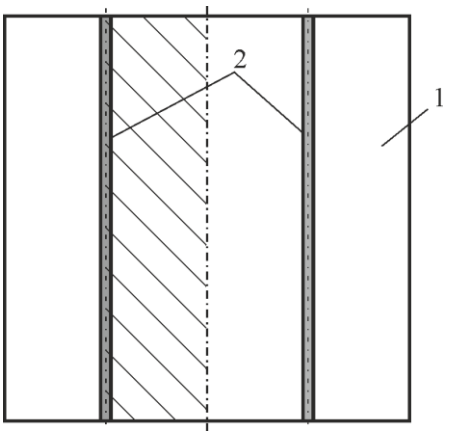

Fig.1. General view of SC (1) with copper ribbons (2). Area for simulation is hatched.

In addition, the low thickness of SC is the reason to consider it as a thermally-thin body and two dimensional temperature field analysis can be accepted.

The simulation area was divided into four zones (Fig. 2, a):

- zone I is the part with the soldered copper ribbon;
- zone II is the soldering region;
- zone III is the unsoldered copper ribbon with solder layer;
- zone IV is the silicon plate.

Cross section of simulated structure with components of each zone is given in Fig.2, b.

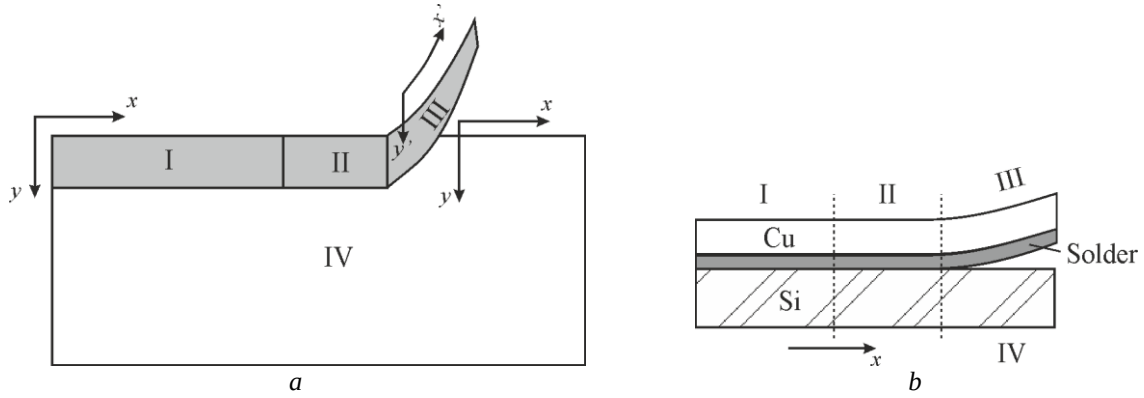

a *b*

Fig. 2. Zones (a) and cross-section (b) of simulated area (a)

All zones except zone II are characterized by convectional heat loses to the ambient air. Zone II was characterized by incoming power only from soldering system. It was accepted that all zones are thermally-thin bodies with averaged physical parameters over zone components. Thermal fluxes, connected with convection and incoming heat from soldering system were described as internal sources. Taking into consideration the melting and crystallization of the solder, the differential equation of thermal conductivity can be written as follows:

$$\frac{c_i\rho_i\,\partial T(x,y,t)}{\partial t}+\frac{q_i\rho_i\,\partial\varepsilon(x,y,t)}{\partial t}=\lambda_i\left(\frac{\partial^2T(x,y,t)}{\partial x^2}+\frac{\partial^2T(x,y,t)}{\partial y^2}\right)+\frac{P_i(x,y,t)}{d_i}, \tag{1}$$

where $d_i=\sum_j d_{ij}$ is the total thickness of zone "*i*";

d_{ij} is the thickness of *j*-component of zone "*i*";

t is the time of soldering process;

$T(x, y, t)$ is the temperature;

$\varepsilon(x, y, t)$ is the melted part of solder, $0 \le \varepsilon(x, y, t) \le 1$;

$P_i(x, y, t)$ is the intensity of internal sources;

c_i, ρ_i, q_i, λ_i are the averaged over components of zone "*i*" specific heat, density, melting heat, and thermal conductivity respectively. They were calculated as follows:

$$\lambda_i=\frac{\sum_j d_{ij}\lambda_{ij}}{d_i};\quad \rho_i=\frac{\sum_j d_{ij}\rho_{ij}}{d_i};$$
$$q_i=\frac{\sum_j qd_{ij}\rho_{ij}}{\sum_j d_{ij}\rho_{ij}};\quad c_i=\frac{\sum_j c_{ij}d_{ij}\rho_{ij}}{\sum_j d_{ij}\rho_{ij}}. \tag{2}$$

where c_{ij}, ρ_{ij}, q_{ij}, λ_{ij} are the specific heat, density, melting heat, and thermal conductivity of *j*-component of zone "*i*" respectively.

Intensity of internal sources was used as follows:

$$P_i(x,y,t)=\begin{cases}\alpha\left(T(x,y,t)-T_a\right), & \text{for zones I, III, and IV;}\\ P, & \text{for zone II.}\end{cases} \tag{3}$$

where α is the heat-transfer coefficient;

T_a is the ambient temperature that considered as a constant during the soldering process;

P is the heat intensity of the soldering system.

Left-hand side of equation (1) consists of two terms, the first of which represents the change of an internal energy due to temperature variation and the second one – due to phase transition. In the model, solder was considered as a one-component substance with one temperature of melting and crystallization (T_m), but not a temperature range as for multicomponent solid solutions. That is why this terms work one after the other.

Boundary conditions between zones I and II, I and IV, and II and IV are the boundary condition of the fourth kind, that was modified due to possibility of phase transition if phase transition temperature is reached:

$$\begin{cases} T\big|_{\zeta=\Gamma-0} = T\big|_{\zeta=\Gamma+0}; \\ \int\left(\left(-\lambda_i \dfrac{\partial T}{\partial \zeta}\Big|_{\zeta=\Gamma-0}\right)+\left(-\lambda_j \dfrac{\partial T}{\partial \zeta}\Big|_{\zeta=\Gamma+0}\right)\right)dt = \left(l_i \rho_i q_i + l_j \rho_j q_j\right)d\varepsilon \end{cases} \quad (4)$$

where ζ is the corresponding coordinate that is perpendicular to the boundary between zones "*i*" and "*j*";

l_i and l_j are the characteristic length of influence of boundary heat flux at melting temperature on phase transition.

Boundary condition between zones II, III and IV was as follow

$$\begin{cases} T\big|_{\zeta=\Gamma-0_{II}} = T\big|_{\zeta=\Gamma+0_{III}} = T\big|_{\zeta=\Gamma+0_{IV}}; \\ \int\left(\left(-\lambda_{II} \dfrac{\partial T}{\partial \zeta}\Big|_{\zeta=\Gamma-0_{II}}\right)+\left(-\lambda_{III} \dfrac{\partial T}{\partial \zeta}\Big|_{\zeta=\Gamma+0_{III}}\right)+\left(-\lambda_{IV} \dfrac{\partial T}{\partial \zeta}\Big|_{\zeta=\Gamma+0_{IV}}\right)\right)dt = \left(l_{II} \rho_{II} q_{II} + l_{III} \rho_{III} q_{III}\right)d\varepsilon. \end{cases} \quad (5)$$

In the model, the value of l_i is dependent on zone number and a boundary temperature:

$$l_i = \begin{cases} h/2, \text{ at } i = \text{I, II, III and } T\big|_{\Gamma} = T_m; \\ 0, \text{ at } i = IV \text{ or } T\big|_{\Gamma} \neq T_m. \end{cases} \quad (6)$$

where h is the spatial step at simulation.

Boundary condition around of the perimeter of simulation area was

$$\frac{\partial T}{\partial \zeta}\Big|_{\zeta=\Gamma} = 0. \quad (7)$$

Initial conditions

$$\begin{cases} T(x, y, 0) = T_a; \\ \varepsilon(x, y, 0) = 0. \end{cases} \quad (8)$$

The boundary-value problem in partial derivatives (1)-(8) was solved numerically by the finite differences method. Due to uncertainty of phase transition in left-hand side of equation (1) at every time step and its dependence on temperature, implicit scheme is not appropriate. That is why explicit scheme for building of equations system was used. It was accepted: spatial step h = 0,5 mm, time step τ = 0,1 ms. For each zone

$$\frac{\lambda_i \tau}{c_i \rho_i h^2} \leq 0{,}1$$

that provides computational stability. Width of copper ribbon was accepted of 2 mm (1 mm in simulation area), soldering spot dimension was accepted 2×2 mm^2. It provided a presence of at least three nodes in each direction for each zone.

Minimization of temperature peaks over T_m was provided in simulation as follows. Initially only power of soldering system was set. Necessity of the system motion to the next position was defined at every time step by state of solder in the last nodes row in the zone II. If in this row the solder was completely melted (ε=1) then soldering system moved the spatial step forward. Examination of solder state and realization of soldering system motion took place until the last nodes row in the zone II would not be melted completely. During the simulation, the number of time steps for each position of soldering system was defined. Simulation was completed when soldering system reached the edge of SC.

Suggested approach gives approximate dependence of position and speed of the soldering system on time that provides Minimization of temperature peaks over T_m. Exact dependences can be obtained only from solutions of reverse heat transfer problem. However, this problem, firstly, is complicated due to its

mathematically incorrectness [14], and, secondly, to set such a problem it is necessary to obtain temperature dependences in internal points, which is undefined due to phase transitions presence.

Physical properties and thickness of the materials used in the simulation are given in Table 1. Solder temperature of phase transition is 183 ºC [11]

Table 1

Physical properties and thickness of the materials used in the simulation [5, 11]

Material	Thickness, μm	Density kg/m^3	Thermal conductivity, W/(m·ºC)	Specific heat, J/(kg·ºC)
Silicon	200	2329	237	816,5
Copper	80	8954	380	383
Solder ($Sn_{63}Pb_{37}$)	40	8410	50,2	230

In Fig. 3 the results of simulation of soldering system position in time at different system powers is given. As follows from Fig. 3, at different powers speed of system is slightly deviate from constant values, but has some delay at the beginning of the process, which is connected with necessity of initial heating from T_a to T_m.

Results of calculation of system speed and initial delay as a function of system heat intensity are given in Fig. 4.

Typical temperature fields at different positions of soldering system at system heat intensity of 40 W/mm^2 are presented in Fig. 5. As follows from Fig. 5, Temperature peaks is very closed to T_m, hence, suggested approach gives the possibility to obtain technological parameters of soldering process, which provides minimal overheating of SC.

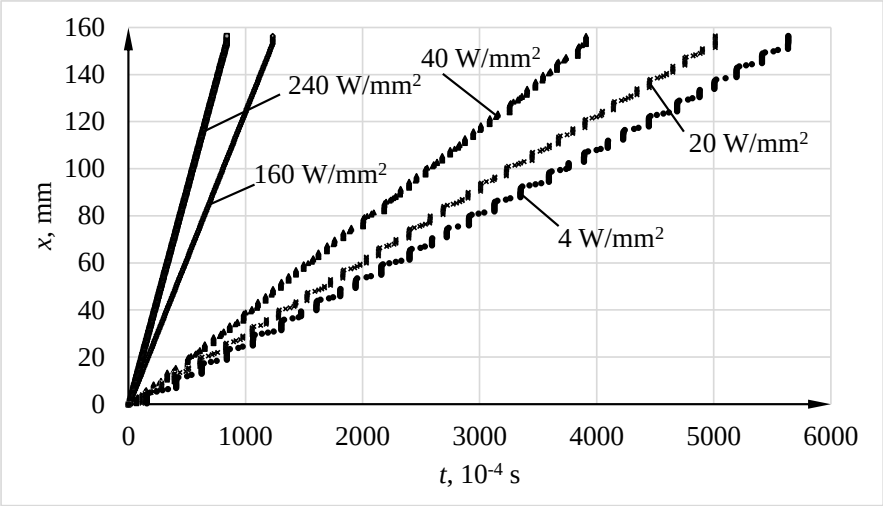

Fig. 3. Results of simulation of soldering system position in time at different system power.

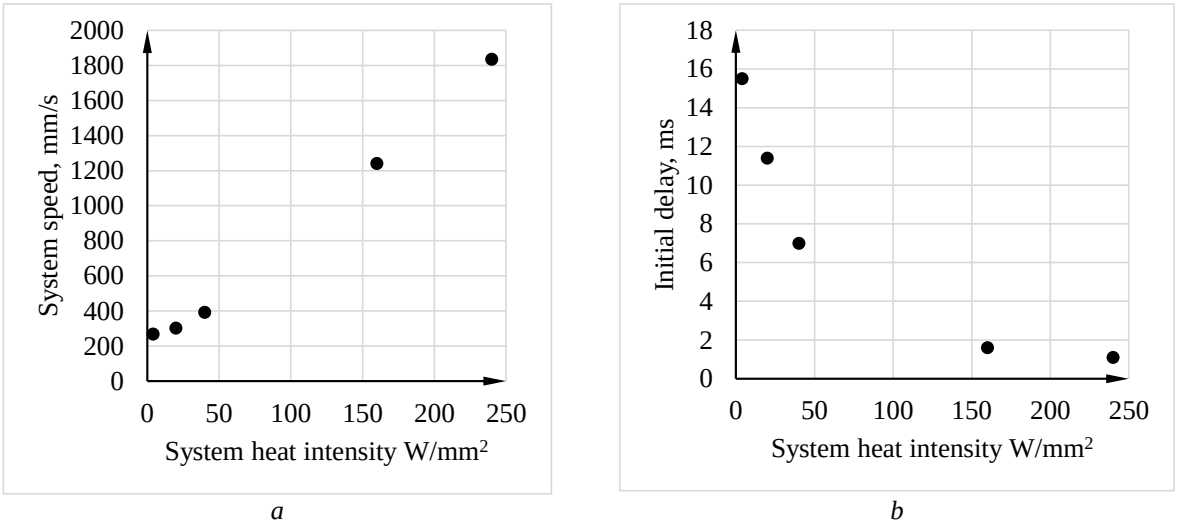

a *b*

Fig. 4. Results of calculation of system speed (a) and initial delay (b) as a function of system heat intensity

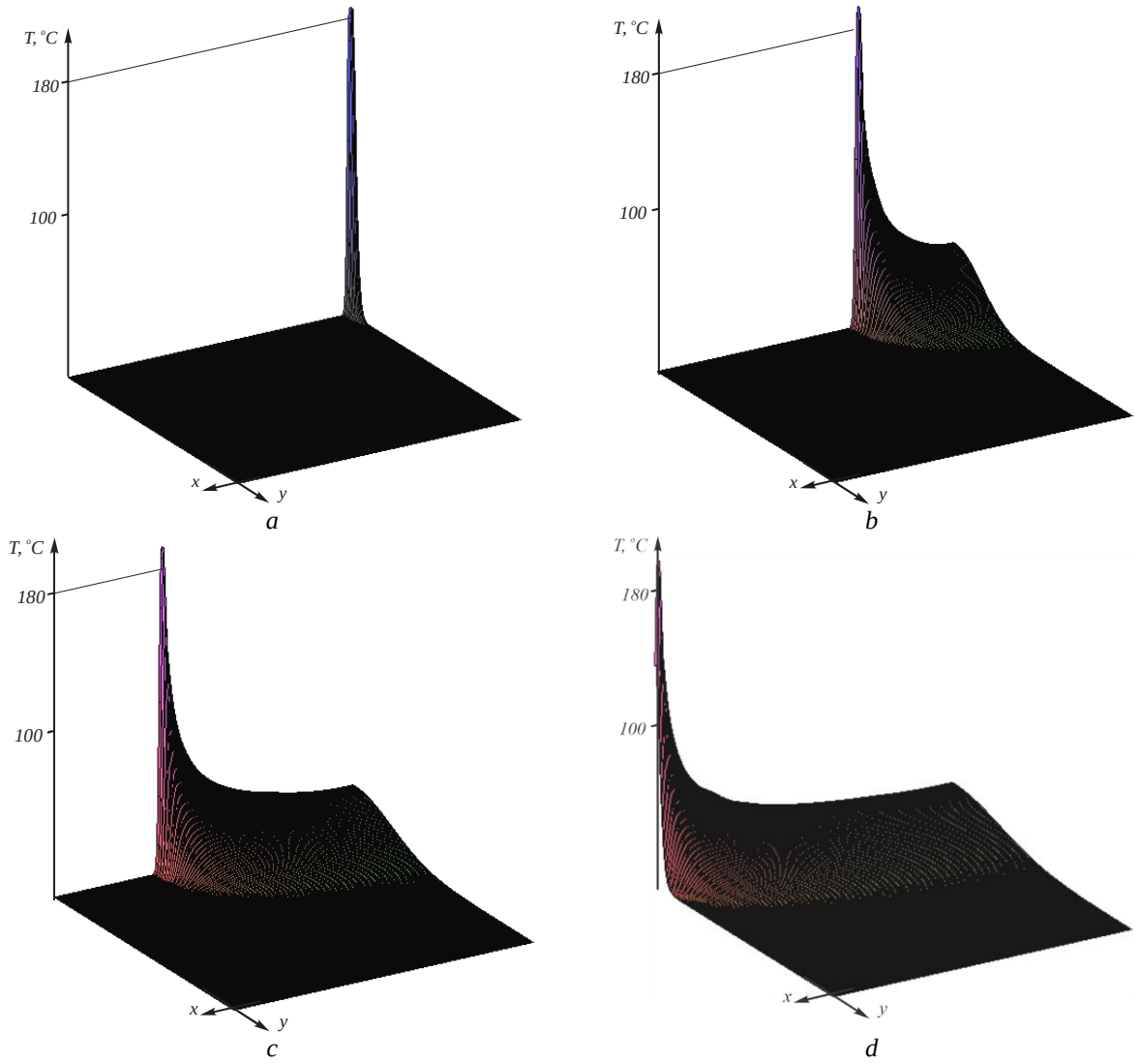

Fig. 5. Temperature fields at different positions of soldering system: a – 0,5 mm; b – 50 mm; c – 100 mm; d – 156 mm

Conclusions

1. The approach for prediction of power and speed dependences in time for spot soldering system during interconnection of crystalline silicon solar cells is develop. Use of this approach gives the possibility to minimize of temperature peaks over solder melting temperature.

2. It was shown, that minimization of overheating can be obtain with practically constant speed of soldering system that is suitable for manufacturing application.

References:

1. Markvart T. Practical Handbook of Photovoltaics: Fundamentals and Applications / T.Markvart L. Castafier. – Elsevier. – 2003. – 984 p.
2. Yang H. The materials characteristic and degradation of cell efficiency for solar grade silicon made by the metallurgical route / H.Yang, H. Wang // Journal of Materials Science. – 46 (4). – 2011. – pp. 1044 – 1048.
3. A review of interconnection technologies for improved crystalline silicon solar cell photovoltaic module assembly / M. Zarmai, N. Ekere, C. Oduoza, E. Amalu // Applied Energy. – 154. – 2015. – pp. 173–182.
4. Gabor A. M. Soldering induced damage to thin Si solar cells and detection of cracked cells in modules/ A. M. Gabor, M. Ralli and S. Montminy // 21st European photovoltaic Solar Energy Conference, Dresden (Germany). – 2006.

5. Lai C.-M. Analysis of the thermal stress and warpage induced by soldering in monocrystalline silicon cells/ C.-M. Lai, C.-H. Su, K.-M. Lin // Applied Thermal Engineering. – 55. – 2013. – pp. 7 – 16.
6. Yang H. Investigation of soldering for crystalline silicon solar cells/ H. Yang, H. Wang, D. Cao // Soldering & Surface Mount Technology. – 28(4). – 2016. – pp. 222 – 226.
7. The impact of yield strength of the interconnector on the internal stress of the solar cell within a module/ Y. Zemen at all. // 25th European Photovoltaic Solar Energy Conference and Exhibition / 5th World Conference on Photovoltaic Energy Conversion, Valencia (Spain). – 2010. – pp. 4073-4078.
8. Hasan K. Thermal deformation analysis of tabbed solar cells using solder alloy and conductive film/ K. Hasan, K. Sasaki // Journal of Mechanical Science and Technology. - 30(7). – 2016. – pp. 3085 – 3095.
9. Low-stress interconnections for solar cells/ P.C. de Jong at all // 20th European Photovoltaic Solar Energy Conference and Exhibition, Barcelona (Spain). – 2005.
10. Britten S. Stress-minimized laser soldering of h-pattern multicrystalline silicon solar cells / S. Britten, A. Olowinsky, A. Gillner // Physics Procedia. – 41. – 2013. – 153 – 163.
11. The finite element modelling of laser soldering for electronic assemblies/ P. M. Beckett at all. // Int. J. Numer. Model. – 15. – 2002. – pp. 265–281.
12. Bunea R. Modeling and Simulation of Pb-free Solder Joints Behavior During Laser Soldering Correlated to the 4P Model/ R. Bunea, P. Svasta, C. Marghescu // 15th International Symposium for Design and Technology of Electronics Packages, Gyula (Hungary). – 2009. – pp. 379 – 382.
13. Numerical Simulation of Laser Soldering about Electronic Connectors / Y. Liu at all. // Advanced Materials Research. -668. – 2013. – pp. 534 – 537.
14. Beck J. Inverse heat conduction. Ill-posed problems/ J. Beck, B Blackwell, C. St. Clair, Jr. – Wiley: New York. – 1985. – 308 p.